

Provenance, tectonic setting and source-area weathering of Mesoproterozoic Kaimur Group, Vindhyan Supergroup, Central India

M. MISHRA^{|1,2|} and S. SEN^{|1|}

^{|1|} Department of Geology, Faculty of Science, Banaras Hindu University
Varanasi-221005

^{|2|} Presently at School of Sciences, Indira Gandhi National Open University
New Delhi-110068. E-mail: meenalbhu@yahoo.co.in

ABSTRACT

The siliciclastic of the Upper Kaimur Group of the Vindhyan Supergroup in Central India have been geochemically studied in order to understand their provenance, paleoweathering conditions and tectonic conditions. A-CN-K (Al_2O_3 -CaO-K₂O) ternary diagram and chemical index of alteration (CIA) values suggest that the granitic source rocks underwent moderate to high degree of chemical weathering under moderate weathering conditions for an extended period of time, or under humid weathering for shorter periods of time. Similar CIA values in all textural types indicate that recycling processes homogenized the shale and sandstone compositions. Various geochemical discriminants and elemental ratios such as $\text{K}_2\text{O}/\text{Na}_2\text{O}$, $\text{Al}_2\text{O}_3/\text{TiO}_2$, SiO_2/MgO , La/Sc, Th/Sc, Zr/Sc, Th/Cr, [Gd/Yb]N and pronounced negative Eu anomalies indicate the rocks to be the product of post-Archean, Proterozoic granitic source, with minor granodioritic input and substantial sediment recycling. The geochemical signatures corroborate their deposition in a subsiding foreland basin over Bundelkhand craton with provenance from south, south westerly Chotanagpur granite gneiss.

KEYWORDS | Kaimur Group. Vindhyan Supergroup. Siliciclastic. Geochemistry. Proterozoic granite. Foreland basin.

INTRODUCTION

Mineralogical and chemical compositions of terrigenous sedimentary rocks are the products of several variables such as provenance, weathering conditions, transport, diagenesis, climate and tectonism (Johnsson and Basu, 1993). In geochemical studies, the major elements and the selected trace elements like Th, Sc, Co, Cr, Zr, Hf, Y including rare earth elements (REEs) and their elemental ratios are sensitive indicators of the source rocks, tectonic

setting, paleoweathering conditions and paleoclimate of the clastic sedimentary rocks (Bhatia, 1983; Bhatia and Crook, 1986; Roser and Korsch, 1986, 1988; McLennan and Taylor, 1991; Johnsson and Basu, 1993; McLennan *et al.*, 1993; Condie, 1993; Nesbitt *et al.*, 1996; Fedo *et al.*, 1997; Cullers and Podkovyrov, 2000, 2002; Bhatt and Ghosh, 2001).

The Vindhyan basin is the largest (presently exposed area 104,000km²) of the Precambrian sedimentary basins

in India (Fig. 1). It comprises a thick (4000m in the thickest parts) sequence of largely unmetamorphosed and undeformed succession of shales, sandstones, limestones, dolostones with subordinate, felsic volcanics and volcanoclastics. They were deposited from before 1.7Ga until shortly after 1Ga (Soni *et al.*, 1987; Sarangi *et al.*, 2004; Gregory *et al.*, 2006; Chakraborty, 2006; Malone *et al.*, 2008). Kajrahat limestone yielded a Pb–Pb age of 1721 ± 90 Ma (Sarangi *et al.*, 2004). Rasmussen *et al.* (2002) and Ray *et al.* (2002) have published consistent U–Pb ages of 1630 and 1631Ma from the Deonar/Porcellanite Formation. Thus the sedimentation in the basin (particularly in the Son valley) started sometime prior to 1721Ma and continued up to ~650Ma. However the upper limit of Vindhyan sedimentation has been bracketed down to 1Ma by Malone *et al.* (2008).

The Lower Vindhyan/Semri Group constitutes the dominant carbonate deposit while the overlying Kaimur Group is majorly a siliciclastic deposit (Table 1). Therefore, the geochemical signatures of the siliciclastic Kaimur Group provide strong evidences of the changing depositional environment, climatic conditions, tectonics and weathering conditions during the Mesoproterozoic era. The purposes of this paper are: i) to report the results of geochemical analysis of sandstone and shales from the Upper Kaimur Group of the Vindhyan Supergroup and ii) to interpret these data in relation to source rock composition, weathering history and tectonic setting of the depositional basin.

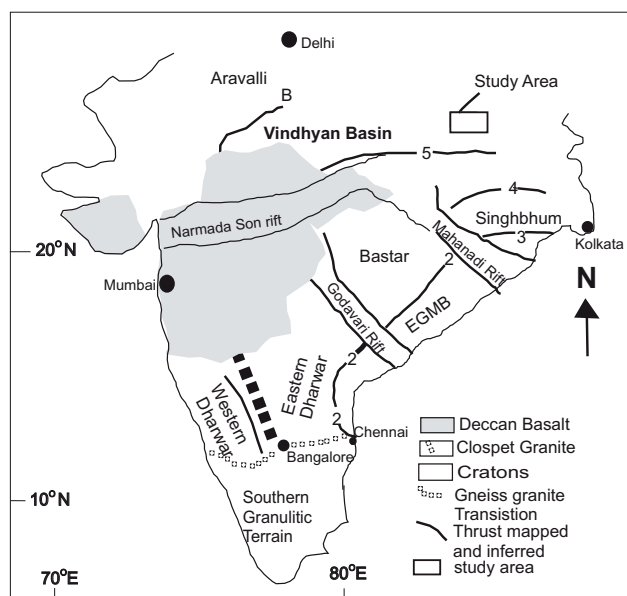


FIGURE 1 | Major cratons and structural features of India (after Naqvi and Rogers, 1987). Major structural features are: 1) Small thrusts in western Dharwar craton; 2) Eastern Ghat front; 3) Sukinda thrust; 4) Singhbhum thrust; 5) Son Valley; and 6) Great Boundary fault. EGMB: Eastern Ghats Mobile Belt.

GEOLOGICAL SETTING

The Vindhyan basin is the repository of the thickest Proterozoic succession in India. The basin overlies the stable Bundelkhand craton of Archean–Early Proterozoic age (Roy, 1988; Chakraborty and Bhattacharya, 1996; Bose *et al.*, 2001; Acharya, 2003). The Vindhyan Supergroup is broadly divided into four Groups—Semri, Kaimur, Rewa and Bhandar—from bottom to top. The Kaimur Group with a thickness up to 400m lies unconformably over the tilted, mildly deformed and partially eroded Rohtas Limestone of the Semri Group. The outcrops of the Semri and Kaimur Groups are exposed in the Son valley area, bounded by the Bundelkhand Granitic Complex (BGC) to the north and by the Mahakoshal Group and Chotanagpur Gneissic Complex in the southern margin (Fig. 2).

Age constraints for the Kaimur Group, derive from the Rb/Sr dating of a kimberlite pipe that intrudes the Kaimur Group at Majhgawan: Crawford and Compston (1970) reported 1140 ± 247 Ma. Kumar *et al.* (1993) reported 1067 ± 31 Ma; more recently Gregory *et al.* (2006) reported 1073.5 ± 13.7 Ma $^{40}\text{Ar}/^{39}\text{Ar}$ on phlogopite in the pipe. The Kaimur Group has been divided into Lower Kaimur Group and Upper Kaimur Group. The Lower Kaimur Group is further divided into the Sasaram Formation, the Ghurma Shale and the Markundi Sandstone. While the Upper Kaimur Group comprises three Formations: Bijaigarh Shale being the lowermost, followed by the Scarp Sandstone and the Dhandraul Sandstone (Auden, 1933; Prakash and Dalela, 1982) (Fig. 2).

The traverse was taken along Markundi-Ghat and Churk sections in the district of Sonbhadra (Fig. 2), where the Upper Kaimur Group (Dhandraul Sandstone, Scarp Sandstone and Bijaigarh Shale) is exposed and Lower Kaimur Group has been cut by the Markundi-Jamwal Fault (Prakash and Dalela, 1982). Thus Bijaigarh Formation directly rests over the Semri Group. The relevant details pertaining to the stratigraphy, lithology and structure of the Upper Kaimur Group exposed in the study area are given in Table 1. The depositional environments for the Dhandraul Sandstone include fluvio-eolian interactive systems; the Lower Kaimur and Bijaigarh Formations and the Scarp Sandstone of Upper Kaimur are interpreted to have been deposited in marine environments, by the earlier workers (Auden, 1933; Morad *et al.*, 1991; Chakraborty and Bose, 1992; Bhattacharya and Morad, 1993; Chakraborty, 1993, 1996; Bose *et al.*, 2001; Paikaray *et al.*, 2008; Mishra and Sen, 2008, 2010).

Dhandraul sandstone

It comprises white, supermature and coarse-grained sandstone. The beds are mostly tabular and laterally con-

TABLE 1 | Stratigraphy of Vindhyan Supergroup showing details of Upper Kaimur Group (after Prakash and Dalela, 1982) with special reference to lithology, structure and samples analyzed

Group	Formation	Lithology	Structures	Samples analysed
Upper Vindhyan	Bhander (139-580)	Dominantly arenaceous (medium to coarse grained) texturally coarsening upward sequence	Large scale cross bedding, through bedding ripple marks	MR-1, MAR-1, MR-2, MAR-2, MAR-16, SPC-13
	Rewa (360-3000)			
	Upper Kaimur	Dhandraul Sandstone (120m)		
		Scarp Sandstone (150m)	Cross bedding, fault gouge and breccia, water seepages, seepages, drag fold, ripple marks, clay galls	MAR-11, MAR-12, MAR-13, MAR-14, MAR-15, SPC-1, SPC-3
		Bijaigarh Shale (25m)	Wavy laminations, Wavy pyritiferous laminae, microbial mats, mud cracks, ripple and wrinkle marks, flute casts, rain prints, adhesion marks	MAR-4, MAR-10 SPC-6, MAR-22 SPC-7, MAR-25, MR-6
	Kaimur (8-400)	Heterogeneous lithology, reddish brown to buff colour shale ranging from siltstone to mudstone. Carbonaceous shales		
Lower Vindhyan/ Semri Group (760-3055m)	Lower Kaimur	Markundi Sandstone	Lower kaimur formations are omitted by Markundi-Jamwal fault (Prakash & Dalela, 1982)	
		Ghurma Shale		
		Sasaram Sandstone		
~~~~~Faulted/Normal contact~~~~~				

tinuous for tens to hundreds of meters with sharp boundaries. The Dhandraul Sandstone exhibits sedimentary structures like large scale cross bedding with long, low-angle foresets which alternate with cosets of parallel laminated sandstone, intersecting trough bedding and ripple marks. The Dhandraul Sandstone is petrographically quartz arenite. The modal analyses data of Dhandraul Sandstone plot in the quartz arenite field and with few in the subarkose field (Sen, 2010) of Folk's (1980) classification. The grains are very well sorted with a high degree of sphericity and roundness. Monocrystalline quartz dominates the polycrystalline variety. Zircon and tourmaline among the heavy minerals, chert and lithic fragments are also present. Lithic fragments often exhibit plutonic igneous textures like granophyric, graphic and perthitic.

Scarp sandstone

This sandstone is of variegated color and medium-grained. It is defined by planar, laterally impersistent erosional surfaces which are invariably carpeted by lensoid bodies of conglomerates consisting of flattened and angular red shale pebbles of intraformational origin. Trough and planar cross bedding are the most prominent sedimentary structures observed. Scarp Sandstone mainly comprises fine to medium sized angular to subangular quartz grains of monocrystalline and polycrystalline nature. Both ferruginous and siliceous cement are present. Quartz grains exhibit moderate sorting, low degree of sphericity and etched surfaces. Chert and lithic fragments and detrital grains of muscovite, zircon and tourmaline are also observed. The modal analyses data of the Scarp

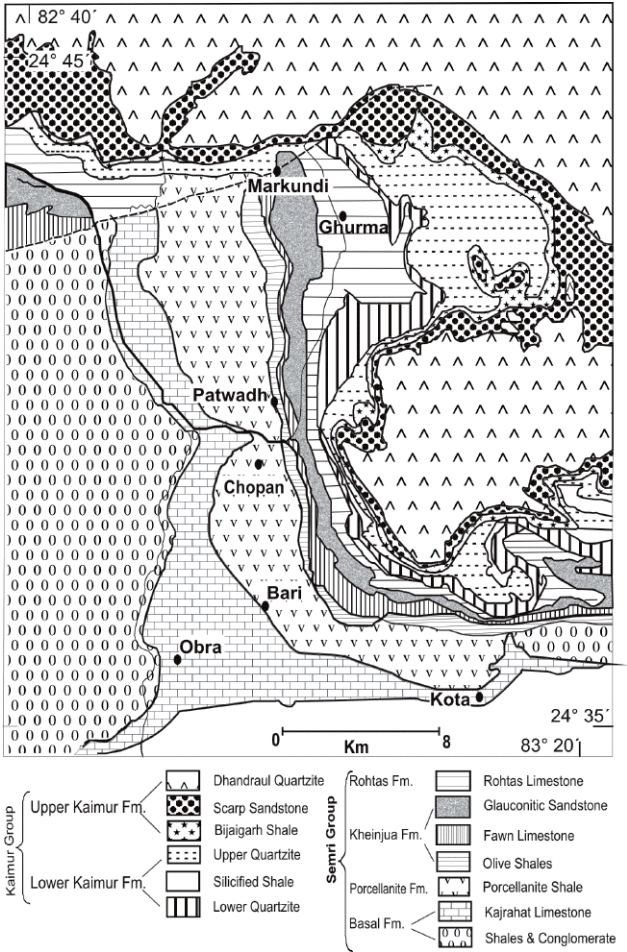


**FIGURE 2** | Detailed geological map of the Vindhyan Supergroup in the Son valley area (modified after Auden, 1933).

Sandstone plot in the sublitharenite and quartz arenite fields (Sen, 2010) of Folk's classification (1980).

### Bijaigarh shale

This Formation exhibits lithological heterogeneities; dominantly made up of shales with wavy laminations and intercalated fine-grained sandstone. Sedimentary structures like ripple marks, wrinkle marks and polygonal mudcracks are commonly observed. The shaly siltstones comprise subangular to subrounded quartz grains with ferruginous cement (usually pyritiferous) and subordinate clayey matrix.

Thus, the siliciclastic of the Upper Kaimur Group exhibit an increase in maturity, both texturally and mineralogically from the Bijagarh shale at the bottom to the Dhandraul sandstone at the top, in a coarsening-upwards sequence.

## SAMPLING AND ANALYTICAL TECHNIQUES

Fresh representative samples were carefully selected on the basis of textural and compositional variations and other distinguishing characteristics from the Markundi-Ghat and Churk section. A total of 21 samples were analyzed for major oxides, trace elements and REE data; eight were from the Bijagarh Shale, seven from the Scarp Sandstone and six from the Dhandraul Sandstone (Table 1). The geochemical data was obtained from Activation Laboratories Ltd., Ancaster, Ontario, Canada using ICP-OES (inductively coupled plasma-optical emission spectrometer) (Model: Thermo-Jarret Ash ENVIRO II) for major elements, whereas ICP-MS (inductively coupled plasma-mass spectrometry) (Model: Perkin Elmer Sciex ELAN 6000) was used to determine trace and REE concentrations. The precision is <5% for all analyzed elements when reported at a 100X detection limit. Several standards, such as SY-3, W-2, DNC-1, BIR-1 and STM-1, were run along with the sandstone and shale samples of the Kaimur Group to check accuracy and precision. Major, trace element and REE data for the shales and sandstones from the three stratigraphic units of the Upper Kaimur Group are tabulated in Tables I and II (Electronic Appendix, available at [www.geologica-acta.com](http://www.geologica-acta.com)) respectively.

## GEOCHEMICAL RESULTS

### Major elements

As expected, the sandstones have a higher  $\text{SiO}_2$  wt%, and correspondingly a lower  $\text{Al}_2\text{O}_3$  wt%, than shales (Table I). All the major elements except  $\text{SiO}_2$  increase in their concentration from the Dhandraul Sandstone to

the Bijagarh Shale. A higher  $\text{K}_2\text{O}/\text{Na}_2\text{O}$  ratio (2.5 to 97) indicates dominance of the feldspar, illite and mica. Bearing in mind that  $\text{Al}_2\text{O}_3$  resides in feldspars, while  $\text{TiO}_2$  in mafic minerals, the  $\text{Al}_2\text{O}_3/\text{TiO}_2$  ratio of 10.6–27 indicates these rocks come from a felsic source. This is also supported by the low values of  $\text{MgO}$ .  $\text{TiO}_2$  is present in rutile. However, a relatively high concentration of  $\text{Fe}_2\text{O}_3$  (0.8–5 wt%) in the Scarp sandstone and Bijagarh shale could be attributed to the presence of ferruginous cement.

Using the geochemical classification diagram of Herron (1988), the Dhandraul Sandstone, Scarp Sandstone and Bijagarh Shale of the Kaimur Group can be compositionally described as quartz arenite, litharenite, sublitharenite and subarkose and shale respectively (Fig. 3). Roddaz *et al.* (2006) have recommended Herron's classification, suggesting it to be a useful additional tool when applied to clastic sedimentary rocks. However, a solid petrographic linkage to chemical parameters in Kaimur siliciclastic has been corroborated with modal analyses data by Sen (2010).

### Trace elements

Ni does not show much variation although Cr (30 to 63 ppm) shows an almost two-fold increase in value from shales to arenites. Ba (22–351 ppm) and Rb (13–145 ppm), which are concentrated in K-feldspars and phyllosilicates, are depleted relative to PAAS (average post-Archean Australian average shale) (Condie, 1993) as well as to average Proterozoic granite. However the Rb values are comparable to average granodiorite. Sr (25–47 ppm) is also greatly depleted when compared with PAAS, average granite and granodiorite. Th (3.3–15 ppm) is depleted with

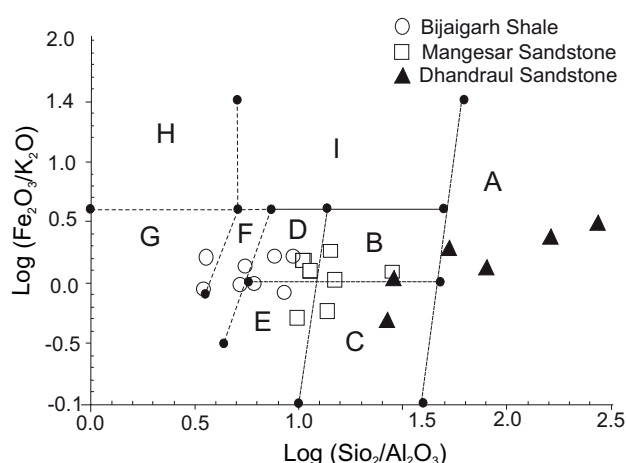


**FIGURE 3** | Plot showing classification of terrigenous sandstones and shales of Upper Kaimur Group. A: Quartz arenite, B: Sublitharenite, C: Subarkose, D: Litharenite, E: Arkose, F: Wacke, G: Shale, H: Fe-Shale, I: Fe-sand. Various fields are according to Herron (1988).



respect to PAAS (14.6ppm) and average granite (18ppm). U (0.9-4.7ppm) is comparable to PAAS (3.1ppm). Zr, Ti, Nb, Hf and Y are preferentially partitioned into melts during fractional crystallization and anatexis (Feng and Kerrich, 1990) and, as a result, they are enriched in felsic rather than mafic rocks. Bijaigarh Shale exhibits a considerable enrichment of Zr (3.2 fold), Y (4.5 fold), Hf (3 fold), Nb (8.3 fold) and Ti (7.4 fold) in comparison to Dhandraul Sandstone. Zr and Hf behave coherently as attested by their high correlation coefficient ( $r=+0.70$ ). Interestingly, the Zr/Hf ratio value for the Bijaigarh Shale (40.7) is almost identical to that in Dhandraul Sandstone (39.2). The behavior of trace elements is similar to that of major elements and they are also affected by quartz dilution, from Dhandraul Sandstone to Bijaigarh Shale.

Additionally, they are thought to reflect provenance composition because of their immobile behavior (Taylor and McLennan, 1985). Zr/Hf ratios for PAAS and average granite are 42 and 34 respectively. Y (3-37ppm) and Nb (1-15ppm) is more comparable to average granodiorite than PAAS or average granite. Various trace element ratios such as Zr/Sc and Th/Sc have been utilized further to determine the provenance of these rocks.

### Rare earth elements

REE abundances of sandstones and shales from the Upper Kaimur Group; vary systematically in relation to lithology and stratigraphy (Table II, Fig. 4). A gradual decrease in  $\Sigma$ REE abundance is observed from the Bijaigarh Shale and Scarp Sandstone to the Dhandraul Sandstone, though with similar REE patterns.  $\Sigma$ REE abundance of Bijaigarh Shale (141-198ppm) is similar to PAAS. Bijaigarh Shale exhibits REE fractionation with  $[La/Yb]_N=7.4$  and  $[Gd/Yb]_N=1.27$ .  $Eu/Eu^*(0.64)$  is similar to PAAS(0.66). The Scarp Sandstone has a lower  $\Sigma$ REE abundance (102-122ppm) than the Bijaigarh Shale and a PAAS with a very similar pattern (Fig. 4). The REE pattern for the Scarp Sandstone appears more fractionated, with  $[La/Yb]_N=8.6$  and  $[Gd/Yb]_N=1.4$  as compared to that of the Bijaigarh Shale. The Dhandraul Sandstone is extremely depleted in REE (31.4-91.2ppm) due to the dilution effect of quartz. It has a considerably fractionated REE pattern with  $[La/Yb]_N=9.93$  and enriched HREE  $[Gd/Yb]_N=1.6$ , in comparison to the underlying Scarp Sandstone and Bijaigarh Shale. The negative Eu anomaly ( $Eu/Eu^*=0.52-0.72$ ) in these rocks is attributed to the Eu-depleted felsic igneous rocks, *i.e.* granites and granodiorite, in the source region. Thus, the overall REE fractionation (*i.e.*,  $[La/Yb]_N$ ) and HREE enrichment increases upwards towards the Dhandraul Sandstone. The REE pattern of the Dhandraul Sandstone and the abundances completely match with those of Proterozoic cratonic sandstones (Condie, 1993).

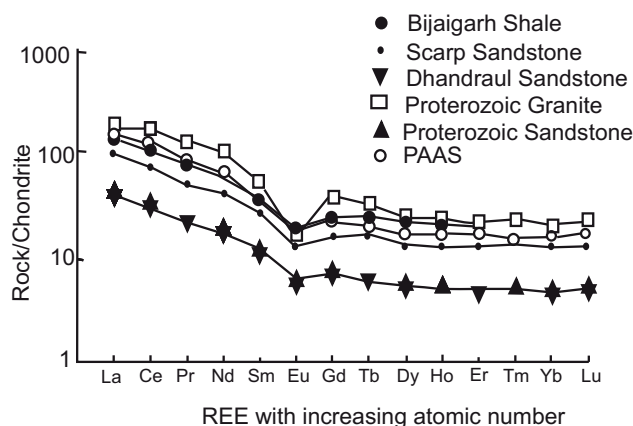


**FIGURE 4** | Chondrite normalized average REE patterns for Upper Kaimur Group siliciclastic, compared with PAAS, Proterozoic granite and Proterozoic Sandstone (Condie, 1993; Taylor and McLennan, 1985).

### GEOCHEMICAL INTERPRETATION

The chemical record of clastic sedimentary rocks is influenced by factors such as source rocks, weathering/recycling, grain-size sorting during transport and sedimentation, and diagenesis and metamorphism (Taylor and McLennan, 1985; McLennan *et al.*, 1990, 1993; Cullers and Podkovyrov, 2000, 2002; Lahtinen, 2000). Thus care must be taken in interpreting the geochemistry of clastic sediments to indicate source composition, as well as to identify the tectonic setting and paleoweathering conditions.

### Weathering intensity-implication for source area composition

The most widely used chemical index to assess the degree of chemical weathering in the source area is the Chemical Index of Alteration (CIA) proposed by Nesbitt and Young (1982). This index can be calculated using molecular proportion:

$$CIA = [Al_2O_3 / (Al_2O_3 + CaO + Na_2O + K_2O)] * 100$$

CIA values of sandstones and shales of the Upper Kaimur Group range from 72 to 87, which is significantly greater than PAAS (70). This suggests that the source rocks of these sedimentary rocks were subjected to intense weathering conditions under a warm humid climate, for a shorter period or moderate degree of chemical weathering for an extended period of time. The ternary plot  $CaO+Na_2O-Al_2O_3-K_2O$  (Fig. 5) is a graphic representation, in order to evaluate the extents of chemical weathering, where unweathered rocks plot along the left side of the plagioclase-K-feldspar line (Nesbitt and Young, 1984). In this plot, the data clusters are found near the A-K

edge, along illite composition, indicating a high extent of weathering of the source rocks.

The determination of source rock composition is an additional advantage of this ternary plot. This could be obtained by backward projection of the weathered sample, parallel to the A-CN line. The point of intersection provides an idea about the plagioclase: K-feldspar ratio of the source rock. Interestingly, samples of all three formations cluster at one point (Fig. 5) indicating their similar extents of chemical weathering. The extrapolation of the line from the weathered sample points indicate the provenance of the rocks of the Upper Kaimur Group to be from average granite.

### Provenance composition-trace elements

The siliciclastic sediments of the Upper Kaimur Group have been subjected to a severe extent of weathering, with sediment recycling and post-depositional K-metasomatism (Mishra and Sen, 2010). Depending solely on major element chemistry to infer provenance would be unreliable, therefore trace elements have been used as the major tool in this respect. Among trace elements, REEs, Th, Sc and high field strength elements (HFSEs) are especially useful for monitoring source area composition (Taylor and McLennan, 1985; Cullers and Podkovyrov, 2002). These elements have very short residence times in the water column, and thus are transferred (almost) quantitatively into the sedimentary record. The ratios between relatively immobile elements such as La/Sc, Th/Sc and Zr/Sc, that are good indicators of provenance.

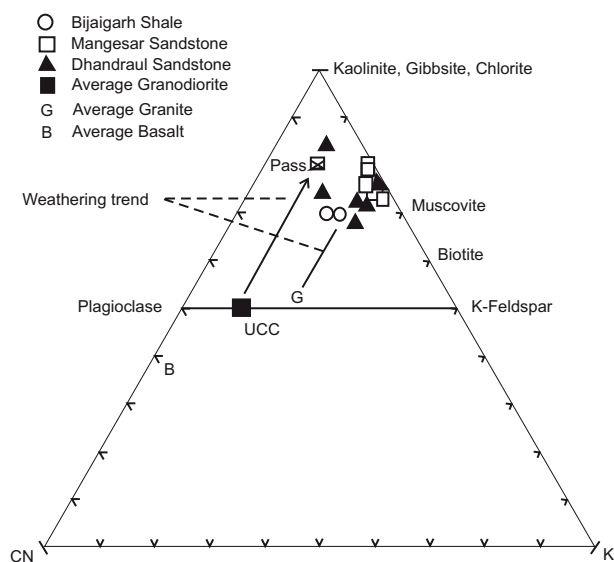


**FIGURE 5** | A-CN-K diagram for Upper Kaimur siliciclastic. A, C, N, K, represent molecular proportions of  $\text{Al}_2\text{O}_3$ ,  $\text{CaO}$ ,  $\text{Na}_2\text{O}$  and  $\text{K}_2\text{O}$  respectively. Average values of G: granite, B: basalt, PAAS and UCC taken from Taylor and McLennan (1985) and Condie (1993).

These ratios for Upper Kaimur sandstones and shales (Table 2) have values comparable to average Proterozoic granite (La/Sc-9.6, Th/Sc-3.6, Zr/Sc-48, Rb/Sr-1.3, La/Ni-3.2, Zr/Hf-34 and  $[\text{La/Yb}]_N$ -9.8, Condie, 1993) as compared to those of PAAS and UCC (Taylor and McLennan, 1985; Rudnik and Gao, 2003).

Th/Sc–Zr/Sc diagram (McLennan *et al.*, 1993) shows that the samples of the Bijaigarh Shale, Scarp Sandstone and Dhandraul Sandstone are clustered around average granite with a minor contribution from granodiorite, confirming a dominantly granitic source (Fig. 6). La and Th are more concentrated in felsic than in mafic igneous rocks, whereas, Co, Sc and Cr are more concentrated in mafic than in felsic igneous rocks. Zirconium is mostly concentrated in zircons, which accumulate during sedimentation while less resistant phases are preferentially destroyed. The Zr/Sc ratio therefore can be used as a tracer for zircon or heavy mineral concentration (Taylor and McLennan, 1985). In first-cycle sediments, Th/Sc ratios show an overall positive correlation with Zr/Sc, depending on the nature of the source rock, whereas Zr/Sc ratios in mature or recycled sediments display considerable variation with little change accompanying in Th/Sc ratio (McLennan *et al.*, 1993), indicating zircon addition due to sediment recycling (Fig. 6). Figure 7 shows the distribution of selected trace and rare earth elements in Kaimur sandstones and shales normalized to that in Proterozoic Granite (Condie, 1993). They show similar patterns but varying abundances due to the dilution effect of quartz. This would favor a weathered crystalline “granitic” source terrain. Thus from the above discussion we can infer that the siliciclastic of the Upper Kaimur Group are derived from a single or similar Proterozoic granitic sources, along with a considerable amount of sediment recycling.

### Implications for tectonic settings

Various workers (Bhatia, 1983; Bhatia and Crook, 1986; Roser and Korsch, 1986, 1988; McLennan *et al.*, 1990) have used the chemical compositions of sandstones to discriminate tectonic settings. On the discrimination diagram of Roser and Korsch (1986) plotting  $\text{K}_2\text{O}$  vs.  $\text{Na}_2\text{O}-\text{SiO}_2$ , Upper Kaimur sandstones and shales plot in the passive margin field, PM (figure not shown here). According to Roser and Korsch (1986), PM sediments are largely quartz-rich sediments derived from plate interiors or stable continental areas and deposited in intra-cratonic basins or on passive continental margins. The plot of Bhatia’s (1983) first and second discriminant functions (DF1 vs. DF2) also favours a passive margin setting (Fig. 8). Collective petrographic and geochemical data strongly suggests that the siliciclastic from Upper

**TABLE 2** | Range of elemental ratios of Upper Kaimur siliciclastic sediments compared to average Proterozoic granite, average Proterozoic sandstone and Upper continental crust. Values taken from; a) Taylor and McLennan (1985); b) Condie, (1993); c) Rudnik and Gao (2003)

Elemental ratios	Range of Upper Kaimur siliciclastics	Average Upper Kaimur siliciclastics	Average Proterozoic granite ^b	Average Proterozoic sandstone ^b	PAAS ^a	Upper continental crust ^c
La/Sc	3.3-10.9	6.9	9.6	4.2	2.37	2.2
Th/Sc	1.1-3.6	2.4	3.6	1.7	0.91	0.75
Th/U	1.2-6.3	3.6	4	3.5	4.7	3.9
Rb/Sr	0.12-4.4	2	1.3	1.2	0.8	0.25
La/Ni	0.5-3.9	2.2	3.2	0.91	0.69	0.65
Cr/Th	2.9-36	6.9	1	2.2	7.5	8.76
Zr/Sc	20.7-68.4	50.2	48	37	13.1	13.7
Zr/Th	9.6-38.5	21.2	13.3	21.1	14.4	18.3
Zr/Hf	27.8-40	37.4	34.2	35.6	42	36.4
Eu/Eu*	0.52-0.72	0.63	0.37	0.68	0.66	0.72
[La/Yb] _N	5.5-12.97	8.5	9.8	8.6	9.2	11.2

^aTaylor and McLennan (1985); ^bCondie (1993); ^cRudnik and Gao (2003)

Kaimur were deposited in a passive margin or stable intracratonic basin.

$DF1 = 0.303 - 0.0447SiO_2 - 0.972TiO_2 + 0.008Al_2O_3 - 0.267Fe_2O_3 + 0.208FeO - 3.082MnO + 0.14MgO + 0.195CaO + 0.719Na_2O - 0.032K_2O + 7.51P_2O_5$

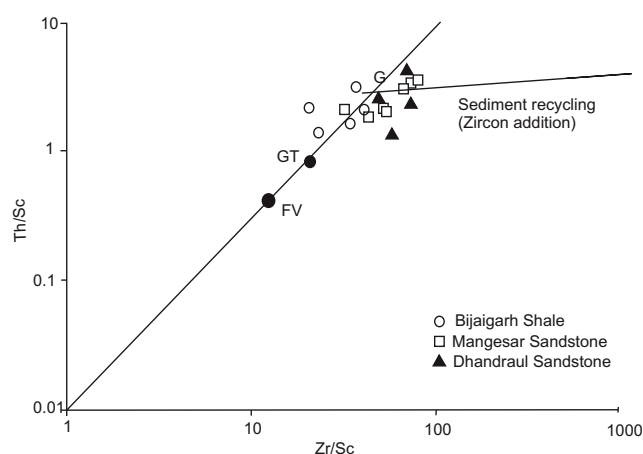
$DF2 = 43.57 - 0.421SiO_2 + 1.988TiO_2 - 0.526Al_2O_3 - 0.551Fe_2O_3 - 1.61FeO + 2.72MnO + 0.881MgO - 0.907CaO - 0.177Na_2O - 1.84K_2O + 7.244P_2O_5$

In addition, the Eu/Eu* values for these rocks is less than 0.85, characteristic of sediments recycled from upper continental crust. The sediments with pronounced negative Eu anomalies <0.85 and [Gd/Yb]_N ratios (1.2-1.9) <2.0 are characteristic of the rocks from the post-Archean period (Taylor and McLennan, 1985; Slack and Stevens, 1994) (Fig. 9). Compositions of the samples overlap each other, well within the field that depict their Proterozoic source. Therefore, the rocks of the Upper Kaimur Group represent a Proterozoic source which was directly exposed to erosion of basement granite and processed through sedimentary recycling.

In Th-Sc-Zr/10 discriminant plot (Bhatia and Crook, 1986), Upper Kaimur sandstones and shale samples fall within the passive margin field (Fig. 10). Bhatia and Crook, (1986) considered that the sedimentary rocks deposited on passive margins, platforms and cratonic basins are characterized by enrichment of LREE over HREE and the presence of a pronounced Eu anomaly on chondrite normalized plots. The crustal source is indicated by the plot positions of average Proterozoic granite (Condie, 1993) relative to the discriminant fields and the composition of the Upper Kaimur Group (Fig. 10).

## DISCUSSION

The Upper Kaimur Group comprising the Bijaigarh Shale, Scarp Sandstone and Dhandraul Sandstone, petrographically and geochemically, range from litharenite and sublitharenite to quartz arenite. Due to the gradational behaviour of the geochemical signatures from Bijaigarh Shale to Dhandraul Sandstone, they should be considered as a single sequence, irrespective of the established field, stratigraphy, although they have been defined as different members (Prakash and Dalela, 1982). CIA values for the shales and sandstones range from 72-88. These values suggest moderate to high extents of chemical weathering

**FIGURE 6** | Th/Sc-Zr/Sc diagram (McLennan et al., 1993) shows that sandstone and shale cluster around average granite with minor contribution from granodiorite. Values of G: granite, B: basalt, GT: granodiorite and FV: felsic volcanic are after Condie (1993).

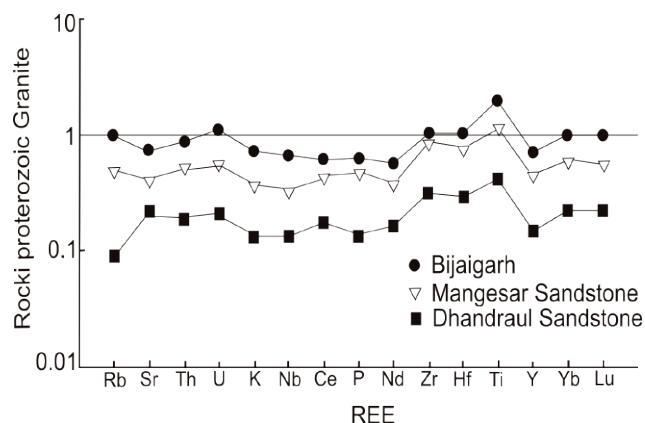


FIGURE 7 | Multielement plot for Upper Kaimur sandstone and shales normalized with Proterozoic granites values from Condie (1993).

under moderate conditions for an extended period of time or intense weathering under hot humid climate for shorter periods of time. The similar CIA values in all three textural types indicate that the recycling processes homogenized the shale and sandstone compositions.

Various major element ratios like  $K_2O/Na_2O$ ,  $Al_2O_3/TiO_2$ ,  $SiO_2/MgO$  and relatively immobile elemental ratios such as  $La/Sc$ ,  $Zr/Sc$ ,  $Th/Sc$  imply source rock to be dominantly granitic. The signatures for addition of zircon perhaps through sediment recycling are also evident (Fig. 6). The geochemical data suggests that the sediments of the Upper Kaimur Group were derived from a post-Archean, Proterozoic granitic source rock deposited in a passive margin type of tectonic setting. Relatively uniform composition, evolved major element compositions (e.g., high  $SiO_2/Al_2O_3$ ,  $K_2O/Na_2O$ ), enrichments of normally incompatible over compatible elements, LREE enrichment, high  $Th/Sc$ ,  $La/Sc$  and

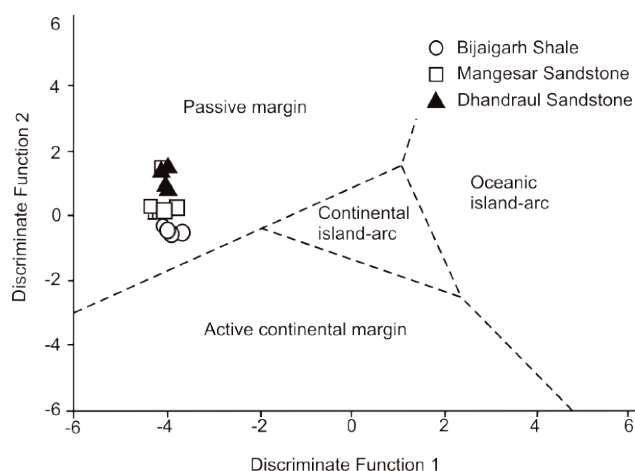


FIGURE 8 | Discrimination function plot of the Upper Kaimur sandstones and shales (after Bhatia, 1983).

high  $Rb/Sr$  ratios ( $>0.5$ ) suggest their derivation from Proterozoic Upper continental crust (PUCC), which constituted the old stable craton (McLennan *et al.*, 1990).

The Vindhyan basin accumulated chemogenic sediments in the lower part (Semri Group) and siliciclastic in the upper part (Kaimur Group). After deposition of the Rohtas Limestone, the Vindhyan basin was affected by the gradual regression of the Vindhyan Sea. This was followed by the initiation of siliciclastic Kaimur sedimentation, which led to the deposition of the Lower Kaimur Quartzite in a tidal flat environment and carbonaceous Bijaigarh Shale in a shallow subtidal and lagoonal environment (Chakraborty and Bose, 1992; Bose *et al.*, 2001).

The Vindhyan basin covers a large part of the northern Indian shield (Fig. 1, 2) and rests on a wide variety of basement rocks including the Banded Gneissic Complex in southeastern Rajasthan, and the Bundelkhand Granite, Bijawar Group, Chotanagpur Granite Gneiss and Mahakoshal Group in central and southeastern India (Nair *et al.*, 1995). The Bundelkhand Gneissic Complex (now in the north of Vindhyan, Son Valley, and basement for the Vindhyan sediments and Mahakoshal metasediments) suffered N-S directed compression due to the northerly subduction of the Bhandara-Bastar craton beneath the Bundelkhand craton (Roy and Prasad, 2003; Bhowmik and Dasgupta, 2004; Roy *et al.*, 2004; Mall *et al.*, 2008; Naganjaneyulu and Santosh, 2010). However, it is argued that sedimentation in the Vindhyan basin initiated at the end of the Delhi-Satpura orogeny as a post-orogenic (post-collision) foreland basin on the Bundelkhand craton, receiving sediments from uplifted fold belts to the south and west (Acharyya, 2003; Chakrabarti *et al.*, 2007; Paikaray *et al.*, 2008). Paleocurrent directions in the Vindhyan sediments are mostly northerly (Banerjee, 1974; Prasad, 1984; Chakraborty, 2006) suggesting that the evolving Satpura orogen might have served as the source for the Vindhyan basin sediments. Chakrabarti *et al.* (2007) indicate changes in provenance with sediments in the Kaimur and Bhandar Groups being derived from more juvenile sources compared to the Semri and Rewa Groups, respectively. This is also supported by changes in  $TDM$  and  $fSm/Nd$  across these boundaries.

The paleocurrent directions in the Vindhyan sediments are mostly northerly and north-westerly (Banerjee, 1974; Prasad, 1984; Bose *et al.*, 2001). Bose *et al.* (2001), based on detailed observation of facies distribution and paleocurrent patterns of the Vindhyan succession in the Son Valley area, have inferred that the sediments were supplied from the southeastern side of the Vindhyan outcrops. The Paleoproterozoic Mahakoshal volcanosedimentary belt and the Chotanagpur Gneiss



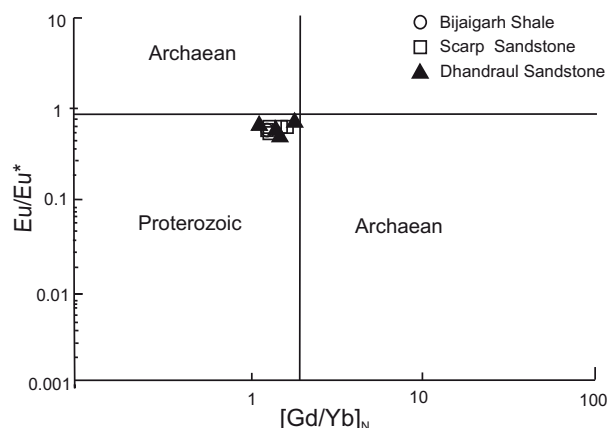


**FIGURE 9** |  $\text{Eu}/\text{Eu}^*$  vs  $[\text{Gd}/\text{Yb}]_N$  diagram indicates the rocks of Upper Kaimur Group to have been derived from Proterozoic provenance. Fields are after Taylor and McLennan (1985), Slack and Stevens (1994).

Complex are situated on the southern and southeastern side of the Vindhyan basin exposures. These seem to be the most likely candidates for the source rocks of the Kaimur group. Therefore, Paleoproterozoic–Mesoproterozoic granite, granodiorite and gneisses of the Mahakoshal Group and Chotanagpur Granite Gneiss (Ghose and Mukherjee, 2000; Singh, 2001) dominantly contributed to the sediments of the Kaimur Group later than the Satpura Orogeny in an intracratonic type of tectonic setting.

## CONCLUSIONS

The provenance of the Kaimur siliciclastic of Son Valley has been assessed using geochemical studies corroborated with petrographic studies. This approach has revealed that the Kaimur sediments were primarily derived from felsic continental sources typical of a craton interior. The CIA values of Upper Kaimur siliciclastic suggest that the source rocks of these sedimentary rocks were subjected to severe and intense weathering conditions under warm humid climate.

$\text{La}/\text{Sc}$ ,  $\text{Th}/\text{Sc}$ ,  $\text{Zr}/\text{Sc}$ ,  $\text{Rb}/\text{Sr}$ ,  $\text{La}/\text{Ni}$ ,  $\text{Zr}/\text{Hf}$ ,  $[\text{La}/\text{Yb}]_N$  and  $\text{Eu}/\text{Eu}^*$  ratios for the Upper Kaimur sedimentary rocks are comparable to average Proterozoic granite. Similarly, A-CN-K,  $\text{Th}/\text{Sc}$ – $\text{Zr}/\text{Sc}$  and  $\text{Th}/\text{Sc}$ – $\text{Zr}/10$  diagrams point to a dominantly granitic source with a minor contribution from granodiorite. The trace elements data indicate that the siliciclastic of the Upper Kaimur Group are derived from a single or similar Proterozoic granitic source of Post-Archaean age. The provenance characteristics suggest that the Kaimur siliciclastic were deposited on a passive margin that received large amounts of mature detritus from the hinterland areas. The Paleoproterozoic Mahakoshal

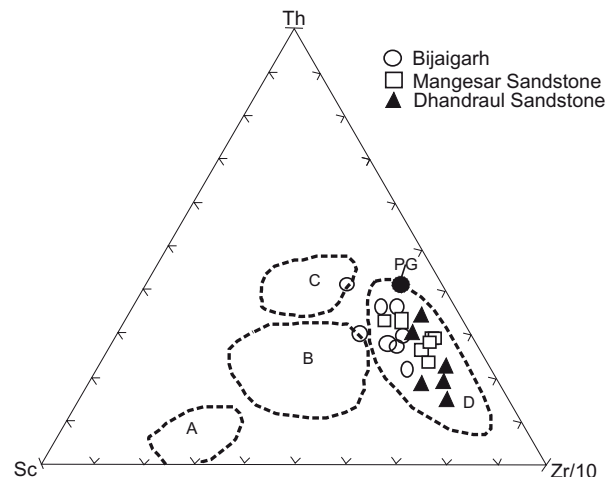


**FIGURE 10** | Ternary Th-Sc-Zr/10 discrimination plot after Bhatia and Crook (1986). A) Oceanic island arc; B) Active continental margin; C) Continental island arc; D) Passive margin. Values for PG-Proterozoic granite are taken from Condie (1993).

belt and Chotanagpur Gneiss Complex are situated on the southern and southeastern side of the Vindhyan basin exposures and they seem to be the potential candidates for the source rocks of the Kaimur group, later to Satpura orogeny.

## ACKNOWLEDGMENTS

MM is grateful to University Grants Commission, New Delhi for financial assistance under the Grant No. F. 31-196/2005 (SR). The authors are thankful to Profs. Robert Cullers, Kansas State University, U.S.A., Abhijit Basu, Indiana University, U.S.A and an anonymous reviewer for their critical comments and suggestions on an earlier version of the manuscript. SS is thankful to the Council of Scientific and Industrial Research, New Delhi for the financial support rendered to her in the form of CSIR-JRF.

## REFERENCES

- Acharyya, S.K., 2003. A plate tectonic model for Proterozoic crustal evolution of Central Indian tectonic zone: Gondwana Geological Magazine, 7 (Special Volume), 9-31.
- Auden, J.B., 1933. Vindhyan sedimentation in the Son Valley, Mirzapur district. Memoir Geological Survey India, 62(II), 141-250.
- Banerjee, I., 1974. Barrier coastline sedimentation model and the Vindhyan example. Contributions to the Earth and Planetary Sciences Golden Jubilee Volume, Quarterly Journal of Mining and Metallurgical Society of India, 46, 101-127.
- Bhatia, M.R., 1983. Plate tectonics and geochemical composition of sandstones. Journal of Geology, 91, 611-627.

- Bhatia, M.R., Crook, K.A.W., 1986. Trace element characteristics of graywackes and tectonic setting discrimination of sedimentary basins. *Contributions to Mineralogy and Petrology*, 92, 181-193.
- Bhatt, M.I., Ghosh, S.K., 2001. Geochemistry of 2.51 Ga old Rampur Group pelites, western Himalayas: Implications from their provenance and weathering. *Precambrian Research*, 108, 1-16.
- Bhattacharya, A., Morad, S., 1993. Proterozoic braided ephemeral fluvial deposits: an example from the Dhandraul Sandstone Formation of the Kaimur Group, Son Valley, Central India. *Sedimentary Geology*, 84, 101-114.
- Bhowmik, S.K., Dasgupta, S., 2004. Tectono-metamorphic evolution of boudin type granulites in the central Indian tectonics zone and in the Aravali-Delhi mobile belt: A synthesis and the future perspectives. *Geological Survey India*, 84 (Special Publications), 227-246.
- Bose, P.K., Sarkar, S., Chakrabarty, S., Banerjee, S., 2001. Overview of the Meso-to Neoproterozoic evolution of the Vindhyan basin, Central India. *Sedimentary Geology*, 142, 395-419.
- Chakrabarti, R., Basu, A.R., Chakrabarti, A., 2007. Trace element and Nd-isotopic evidence for sediment sources in the mid-Proterozoic Vindhyan Basin, central India. *Precambrian Research*, 159, 260-274.
- Chakraborty, C., 1993. Morphology, internal structure and mechanics of small longitudinal (seif) dunes in an aeolian horizon of Proterozoic Dhandraul Quartzite, India. *Sedimentology*, 40, 79-85.
- Chakraborty, C., 1996. Sedimentary records of erg development over a braidplain: Proterozoic Sandstone. *Memoir of the Geological Society of India*, 36, 77-99.
- Chakraborty, C., 2006. Proterozoic intracontinental basin: the Vindhyan example. *Journal of Earth System Science*, 115(1), 3-22.
- Chakraborty, C., Bhattacharyya, A., 1996. The Vindhyan basin: an overview in the light of current perspectives. *Memorial Geological Society of India*, 36, 301-312.
- Chakraborty, C., Bose, P.K., 1992. Morphology, internal structure and mechanics of small longitudinal (seif) dunes in an aeolian horizon of the Proterozoic Dhandraul Quartzite, India. *Sedimentology*, 40, 79-85.
- Condie, K.C., 1993. Chemical composition and evolution of the upper continental crust: contrasting results from surface samples and shales. *Chemical Geology*, 104, 1-37.
- Crawford, A.R., Compston, W., 1970. The age of Vindhyan system of Peninsular India. *Journal of the Geological Society of London*, 125, 351-371.
- Cullers, R.L., Podkovyrov, V.M., 2000. Geochemistry of the Mesoproterozoic Lakhanda shales in southeastern Yakutia, Russia: Implications for mineralogical and provenance, and recycling. *Precambrian Research*, 104, 77-93.
- Cullers, R.L., Podkovyrov, V.N., 2002. The source and origin of terrigenous sedimentary rocks in the Mesoproterozoic Uig group, south-eastern Russia. *Precambrian Research*, 117, 157-183.
- Fedo, C.M., Young, G.M., Nesbitt, H.W., Hanchar, J.M., 1997. Potassic and sodic metasomatism in the Southern Province of the Canadian Shield: Evidence from the Paleoproterozoic Serpent Formation, Huronian Supergroup. *Canada Precambrian Research*, 84, 17-36.
- Feng, R., Kerrich, R., 1990. Geochemistry of fine-grained clastic sediments in the Archean Abitibi greenstone belt, Canada. Implications for provenance and tectonic setting. *Geochimica Cosmochimica Acta*, 54, 1061-1081.
- Folk, R.L., 1980. *Petrology of Sedimentary rocks*. Austin (Texas, U.S.A.), Hemphill Publishing Company, 182pp.
- Ghose, N.C., Mukherjee, D., 2000. Chotanagpur gneiss-granulite complex. In: Trivedi, A.N., Sarkar, B.C., Ghose, N.C., Dhar, Y.R. (eds.). *Geology and Mineral Resources of Bihar and Jharkhand Institute of Geoexploration and Environment Monograph*. Indian School of Mines, Dhanbad, Platinum Jubilee Commemoration Volume, 33-58.
- Gregory, L.C., Meert, J.G., Pradhan, V., Pandit, M.K., Tamrat, E., Malone, S.J., 2006. A paleomagnetic and geochronologic study of the Majhgawan kimberlite, India: Implications for the age of the Upper Vindhyan Supergroup. *Precambrian Research*, 149, 65-75.
- Herron, M.M., 1988. Geochemical classification of terrigenous sands and shales from core or log data. *Journal of Sedimentary Petrology*, 58, 820-829.
- Johnsson, M.J., Basu, A., 1993. Processes Controlling the Composition of Clastic Sediments. *Geological Society of America*, 284(Special Paper), 342pp.
- Kumar, A., Kumari, P., Dayal, A.M., Murthy, D.S.N., Gopalan, K., 1993. Rb-Sr ages of Proterozoic kimberlites of India: evidence for contemporaneous emplacements. *Precambrian Research*, 62, 227-237.
- Lahtinen, R., 2000. Archean-Proterozoic transition: geochemistry, provenance and tectonic setting of metasedimentary rocks in central Fennoscandian Shield, Finland. *Precambrian Research* 104(3-4), 147-174.
- Mall, D.M., Reddy, P.R., Mooney W.D., 2008. Collision tectonics of the Central Indian Suture zone as inferred from a deep seismic sounding study. *Tectonophysics*, 460, 116-123.
- Malone, S., Meert, J., Banerjee, D.M., Pandit, M., Tamrat, E., Kamenov, G.D., Pradhan, V., Sohl, L.E., 2008. Paleomagnetism and detrital zircon geochronology of the Upper Vindhyan Sequence, Son Valley and Rajasthan, India: A ca. 1000Ma closure age for the Purana Basins? *Precambrian Research*, 164, 137-159.
- McLennan, S.M., Taylor, S.R., 1991. Sedimentary rocks and crustal evolution: Tectonic setting and secular trends. *Journal of Geology*, 99, 1-21.
- McLennan, S.M., Hemming, S., McDaniell, D.K., Hanson, G.N., 1993. Geochemical approaches to sedimentation, provenance, and tectonics. In: Johnsson, M.J., Basu, A. (eds.). *Processes Controlling the Composition of Clastic Sediments*. Geological Society of America, Special Paper, 285, 21-40.
- McLennan, S.M., Taylor, S.R., McCulloch, M.T., Maynard, J.B., 1990. Geochemical and Nd-Sr isotopic composition of deep-

- sea turbidites: crustal evolution and plate tectonic associations. *Geochimica et Cosmochimica Acta*, 54, 2015-2050.
- Meenal, M., Shinjana, S., 2010. Geochemical signatures of Mesoproterozoic siliciclastic rocks of Kaimur Group, Vindhyan Supergroup, Central India. *Chinese Journal of Geochemistry*, 29(1), 21-31.
- Meenal, M., Shinjana, S., 2008. Geochemistry and Origin of Proterozoic porcellanitic shales from Chopan, Vindhyan basin, India. *Indian Journal of Geology*, 80(1-4), 157-171.
- Morad, S., Bhattacharya, A., Al-Aasam, L.S., 1991. Diagenesis of quartz in Late Proterozoic Kaimur Sandstones, Son Valley, India. *Sedimentary Geology*, 73, 209-225.
- Naganjaneyulu, K., Santosh, M., 2010. The Central India Tectonic Zone: A geophysical perspective on continental amalgamation along a Mesoproterozoic suture. *Gondwana Research*, Vol. 18(4): 547-564.
- Nair, K.K.K., Jain, S.C., Yeddekar, D.B., 1995. Stratigraphy, structure and geochemistry of the Mahakoshal greenstone belt. *Memoir of the Geological Society of India*, 31, 403-432.
- Naqvi, S.M., Rodgers, J.J.M. 1987. *Precambrian Geology of India*. Oxford Monographs on Geology and Geophysics, No. 6. Oxford University Press, 223pp.
- Nesbitt, H.W., Young, G.M., 1982. Early Proterozoic climates and plate motions inferred from major elements of lutites. *Nature*, 299, 715-717.
- Nesbitt, H.W., Young, G.M., 1984. Prediction of some weathering trends of plutonic and volcanic rocks based on thermodynamics and kinetic consideration. *Geochimica et Cosmochimica Acta*, 48, 1223-1234.
- Nesbitt, H.W., Young, G.M., McLennan, S.M., Keays, R.R., 1996. Effects of chemical weathering and sorting on the petrogenesis of siliclastic sediments, with implications for provenance studies. *Journal of Geology*, 104, 525-542.
- Paikaray, S., Banerjee, S., Mukherji, S., 2008. Geochemistry of Shales from the Paleoproterozoic to Neoproterozoic Vindhyan Supergroup: Implications on Provenance, Tectonics and Paleoweathering. *Journal of Asian Earth Sciences*, 32(1), 34-48.
- Prakash, R., Dalela, S., 1982. *Geology of Vindhyachal*. A volume in honour of Prof. R.C. Mishra. New Delhi (India), Hindustan Publishing Corporation., 55-79.
- Prasad, B., 1984. Geology, sedimentation and paleogeography of the Vindhyan Supergroup, S.W. Rajasthan. *Memoir of the Geological Survey of India*, 116(1), 1-107.
- Rasmussen, B., Bose, P.K., Sarkar, S., Banerjee, S., Fletcher, I.R., McNaughton, N.J., 2002. 1.6Ga U-Pb Zircon ages of Chorhat sandstone, Lower Vindhyan, India: possible implication for early evolution of animals. *Geology*, 30, 103-106.
- Ray, J.S., Martin, M.W., Veizer, J., Bowring, S.A., 2002. U-Pb zircon dating and Sr isotope systematics of Vindhyan Supergroup, India. *Geology*, 30, 131-134.
- Roddaz, M., Viers, J., Brusset, S., Baby, P., Boucayrand, C., Herail, G., 2006. Controls on weathering and provenance in the Amazonian foreland basin: insights from major and trace element geochemistry of Neogene Amazonian sediments. *Chemical Geology*, 226, 31-65.
- Roser, B.P., Korsch, R.J., 1986. Determination of tectonic setting of Sandstones–mudstone suites using SiO₂ content and K₂O/Na₂O ratio. *Journal of Geology*, 94, 635-650.
- Roser, B.P., Korsch, R.J., 1988. Provenance signatures of sandstone–mudstone suites determined using discriminant function analysis of major-element data. *Chemical Geology*, 67, 119-139.
- Roy, A., Prasad, M.H., 2003. Tectonothermal events in Central Indian Tectonic Zone (CITZ) and its implications in Rodinian crustal assembly. *Journal of Asian Earth Sciences*, 22, 115-129.
- Roy, A., Kagami, H., Yoshida, M., Roy, A., Bandyopadhyay, B.K., Chattopadhyay, A., 2004. Rb/Sr and Sm/Nd dating of different metamorphic events from the Sausar mobile belt, central India; implications for Proterozoic crustal evolution. *Journal of Asian Earth Sciences*, 26, 61-76.
- Roy, A.B., 1988. Stratigraphic and tectonic framework of the Aravalli mountain range. In: Roy, A.B. (ed.). *Precambrian of the Aravalli Mountain*. Rajasthan (India), *Memoir of Geological Society of India*, 3-31.
- Rudnick, R.L., Gao, S., 2003. Composition of the continental crust, *Treatise of Geochemistry*, 3, 1-64.
- Sarangi, S., Gopalan, K., Kumar, S., 2004. Pb-Pb age of earliest megascopic, eukaryotic alga bearing Rohtas Formation, Vindhyan Supergroup, India: implications for Precambrian atmospheric oxygen evolution. *Precambrian Research*, 132, 107-121.
- Sen, S., 2010. Geochemistry and provenance of the siliciclastic from Kaimur Group, Vindhyan Supergroup, Mirzapur and Sonbhadra districts, Uttar Pradesh, India. Doctoral Thesis. Varanasi, Banaras Hindu University, 221pp.
- Singh, S.P., 2001. Early Precambrian stratigraphy of the Chotanagpur province. *Precambrian Crustal Evolution and Metallogeny of India*, Singh, S.P. (eds.), South Asian Association of Economic Geologists, 127-137.
- Slack, J.F., Stevens, P.J., 1994. Clastic metasediments of the Early Proterozoic Broken Hill Group, New South Wales, Australia: geochemistry, provenance, and metallogenic significance. *Geochimica et Cosmochimica Acta*, 58, 3633-3652.
- Soni, M.K., Chakraborty, S., Jain, V.K., 1987. Vindhyan Supergroup—a review. *Memoir of the Geological Society of India*, 6, 87-138.
- Taylor, S.R., McLennan, S. 1985. *The Continental Crust: Its composition and Evolution*. Oxford, Blackwell, 312pp.

Manuscript received September 2009;

revision accepted March 2011;

published Online February 2012.

ELECTRONIC APPENDIX

TABLE I | Major oxide and trace element composition of sandstones and shales from Upper Kaimur Group

Major Element (Wt%)	Bilalgarh shale				Scarp Sandstone				Dhandraul Sandstone												
	MR-6	MR-8	22-mar	SPC 7	MAR-4	MAR25	SPC 6	MAR-10	MAR-11	SPC 1	SPC 3	MAR-13	MAR-12	MAR-15	MAR-14	MAR-16	SPC-13	MR-1	MR-2	MAR-1	MAR-2
SiO ₂	62.1	65.2	72.5	72.5	74.8	78.4	81.7	81.9	82.5	84.5	86.1	86.3	88.3	88.4	93.8	94.1	96.3	96.5	97.2	98.6	99.4
TiO ₂	0.66	0.66	0.56	0.53	0.61	0.45	0.42	0.44	0.44	0.34	0.35	0.28	0.24	0.23	0.31	0.21	0.12	0.05	0.10	0.04	0.04
Al ₂ O ₃	17.7	16.0	13.7	13.1	12.1	10.2	9.7	8.6	7.95	8.61	7.58	6.1	5.96	6.46	3.29	3.51	3.28	1.2	1.84	0.61	0.36
Fe ₂ O ₃ (T)	3.8	5.0	3.5	4.7	3.3	4	2.23	3.6	3.79	1.10	2.36	3	1.72	0.8	0.9	0.5	0.3	0.3	0.9	0.4	0.3
MnO	0.0	0.1	0.0	0.0	0.0	0.02	0.02	0.01	0.03	0.02	0.025	0.006	0.004	0.004	0.004	0.004	0.014	0.01	0.02	0.004	0.002
MgO	2.2	3.1	1.2	1.2	0.7	0.91	0.92	0.4	0.88	0.64	0.78	0.21	0.27	0.15	0.09	0.1	0.15	0.05	0.28	0.02	0.009
CaO	1.2	1.0	0.2	0.1	0.1	0.14	0.11	0.06	0.09	0.08	0.11	0.04	0.07	0.03	0.03	0.03	0.07	0.04	0.04	0.02	0.009
Na ₂ O	0.5	0.8	0.1	0.1	0.1	0.11	0.14	0.04	0.05	0.10	0.1	0.03	0.02	0.02	0.01	0.01	0.09	0.08	0.07	0.009	0.009
K ₂ O	4.5	3.5	3.8	3.6	3.4	2.5	2.7	2.2	2.51	2.17	1.89	1.64	1.64	1.38	0.74	0.97	0.33	0.2	0.49	0.18	0.11
P ₂ O ₅	0.1	0.04	0.1	0.1	0.04	0.03	0.02	0.06	0.07	0.02	0.03	0.03	0.03	0.04	0.04	0.03	0.013	0.02	0.03	0.02	0.03
LOI	nd	nd	3.9	4.0	3.6	3.56	2.28	2.72	1.96	1.49	1.28	1.71	1.58	1.68	0.85	0.74	0.4	nd	nd	0.08	0.03
Total	92.7	95.2	95.7	96.1	98.6	96.7	97.98	100.1	100.3	97.56	99.34	99.38	99.88	99.18	100.1	100.1	100.68	98.38	100.93	100	100.3
CIA	74.3	75.2	77	77	77.2	78.9	76.5	78.8	75	78.6	78.3	78.1	77.5	81.9	80.8	77.7	87	78.9	75.4	74.5	72.1
SiO ₂ /Al ₂ O ₃	3.5	4.1	5.3	5.5	6.2	7.7	8.5	9.5	10.4	9.8	11.4	14.2	14.8	13.7	28.5	26.8	29.4	80.4	52.8	162	276
K ₂ O/Na ₂ O	8.9	4.2	31.5	26	48.4	22.5	19.4	55.5	50.2	21.7	19	54.7	82	69	74	97	3.7	2.5	7	20	12.2
K ₂ O/Al ₂ O ₃	0.25	0.22	0.28	0.28	0.28	0.24	0.28	0.26	0.32	0.25	0.25	0.27	0.28	0.21	0.22	0.28	0.10	0.17	0.27	0.30	0.31
Al ₂ O ₃ /TiO ₂	26.9	24.2	24.5	24.8	19.8	22.6	23.0	19.8	18.0	25.3	21.7	21.6	24.9	27.7	10.6	17.0	27.3	24.0	18.4	13.9	8.8
Trace elements (ppm)																					
Ba	435	350	437	446	342	282	301	217	259	167	186	92	110	99	71	45	21	18	19	16	17
Sr	65	55	59	40	51	34	26	30	36	39	41	49	44	64	60	40	19	24	28	17	25
Zr	255	240	259	180	231	274	233	244	309	219	228	217	172	129	135	141	58	68	58	49	73
Y	32	32	31	32	31	37	30	21	27	24	23	18	16	17	13	10	7	7	6	3	6
Ni	16	19	13	21	20	26	10	20	20	6	8	20	20	20	20	20	11	10	25	20	20
Cr	59	59	nd	nd	60	nd	nd	60	70	nd	nd	50	60	80	70	90	11	80	70	90	50
Hf	5.2	5.1	9.3	6.1	6.2	10.8	7.3	6.3	8.3	5.9	5.6	5.5	4.5	3.1	3.5	3.7	1.6	1.5	1.2	2.1	2.2
Sc	9.3	9.1	7.2	8.7	10.2	6.7	6.8	7.1	6.2	3.2	2.9	4.1	4.2	4.1	2.2	2.3	1.2	1.2	1.1	1.2	1.1
Nb	15.2	15.3	15.2	14.3	11.1	11.7	11.3	8.2	8.1	8.7	9.2	5.2	4.3	4.3	5.1	3.2	2.2	1.4	1.3	0.9	0.9
Th	20.3	10.2	21.6	18.7	13.8	14.1	11.2	11.5	13.1	10.1	10.3	8.2	7.3	8.3	6.3	8.2	1.5	2.5	2.9	2.5	2.3
U	7.1	5.3	5.7	3.8	3.5	4.3	6.2	2.7	2.9	3.3	2.7	2.3	1.9	2.3	1.5	1.3	1.3	0.8	0.8	0.6	0.7
Rb	169	155	180	158	151	123	115	106	113	90	84	74	73	59	31	38	14	8	9	7	3
Th/Sc	2.22	1.11	3.08	2.15	1.38	2.10	1.62	1.64	2.18	3.38	3.60	2.00	1.83	2.08	3.00	4.10	1.50	2.5	2.9	2.5	2.3
Th/U	2.86	2.00	3.8	5.0	3.9	3.5	1.8	4.3	4.5	3.1	3.8	3.5	3.8	3.6	4.0	6.3	1.2	3.13	3.63	4.2	3.3
Th/Cr	0.34	0.17	nd	nd	0.23	nd	nd	0.19	0.19	nd	nd	0.16	0.12	0.10	0.09	0.09	nd	0.03	0.04	0.03	0.05
Zr/Sc	27.4	26.4	36.0	20.7	22.6	40.8	34.3	34.4	49.8	68.4	79.2	52.9	41.0	31.5	61.4	61.3	48.2	56.7	52.7	40.8	66.4
Rb/Sr	2.6	2.8	3	4.0	3	3.6	4.4	3.5	3.1	2.3	2	1.5	1.7	0.92	0.52	0.95	0.7	0.33	0.32	0.41	0.12
La/Sc	3.3	4.0	5.8	4.4	3.6	5.2	4.4	4.2	5.6	7.8	8.1	5.6	5.4	6.4	9.1	10.9	9.9	9.88	9.7	6.9	9.2
Ba/Sc	48.3	38.9	62.4	51.2	34.2	42.0	44.4	31.0	43.2	55.7	64.7	23.0	27.5	24.8	35.5	22.5	21.0	18	19	16.0	17.0
Ba/Sr	6.69	6.36	7.4	11.2	6.7	8.35	11.58	7.2	7.2	4.3	4.54	1.9	2.5	1.5	1.2	1	1.11	0.75	0.68	0.94	0.68
Zr/Hf	49.0	47.1	27.8	29.8	37.3	25.5	32.1	38.7	37.2	36.9	40.5	39.5	38.2	41.6	38.6	38.1	36.8	45.3	48.3	23.3	33.2
La/Ni	0.0	0.0	0.0	0.0	0.0	0.0	0.0	0.0	0.0	0.0	0.0	0.0	0.0	0.0	0.0	0.0	0.0	0.0	0.0	0.0	0.0
Cr/Th	2.9	5.8	nd	nd	4.3	nd	nd	5.2	5.3	nd	nd	6.1	8.2	9.6	11.1	11.0	nd	32.0	24.1	36.0	21.7
Zr/Th	12.6	23.5	12.0	9.6	16.7	19.4	20.8	21.2	23.6	21.6	22.0	26.5	23.6	15.5	21.4	17.2	38.5	27.2	20.0	19.6	31.7



TABLE II | Rare Earth elements concentrations of sandstones and shales from Upper Kaimur Group

REE (in ppm)	Bijaiagarh shale			Scarp Sandstone					Dhandraul Sandstone												
	MR-6	MR-8	MAR-22	SPC 7	MAR-4	MAR-25	SPC 6	MAR-10	MAR-11	SPC 1	SPC 3	MAR-13	MAR-12	MAR-15	MAR-14	MAR-16	SPC-13	MAR-1	MAR-2	MR-1	MR-2
La	29.5	35.8	40.4	38.5	35.6	35.1	29.6	29.7	33.5	23.5	23.2	22.3	21.4	25.6	18.2	21.7	9.9	6.9	9.2	9.882	9.7
Ce	59.8	69.4	82.3	75.6	70	70.4	60	60.6	69.5	46	46.4	43.6	42.7	50.9	38.4	37.5	21.8	13.4	19	21.828	21.9
Pr	6.42	7.85	8.61	8.13	7.83	8.03	6.32	6.43	7.41	4.76	4.81	4.74	4.65	5.63	4.24	3.69	2.17	1.4	1.94	2.167	2.3
Nd	24.3	30.1	35.5	33.1	30.2	34	25.8	24.1	28.2	19.2	19.9	17.8	18.1	21.7	16.5	12.4	8.97	5.2	7.3	8.972	9.1
Sm	4.6	5.9	6.9	7	6	7.4	5.5	4.4	5.4	4.8	4.8	3.4	3.5	4.3	3.4	2.1	2.1	1	1.6	2.056	2.1
Eu	0.95	1.3	1.24	1.4	1.2	1.5	1.1	0.84	1	0.71	0.78	0.68	0.69	0.86	0.63	0.39	0.43	0.16	0.27	0.429	0.431
LREE	125.6	150.4	175.0	163.6	150.7	156.4	128.2	126.1	145.0	98.9	99.8	92.5	91.0	109.0	81.4	77.8	45.3	28.1	39.3	45.3	45.5
Gd	4.1	5.6	5.4	6	5.5	6.4	4.4	3.9	5	3.1	3.04	3.3	3	3.8	2.8	1.7	1.6	0.9	1.4	1.61	1.62
Tb	0.9	1	1	1.1	0.9	1.3	0.8	0.7	0.9	0.5	0.5	0.6	0.5	0.6	0.5	0.3	0.24	0.2	0.2	0.242	0.243
Dy	4.2	5.2	6.03	6.5	5.1	8.2	4.6	4	5.1	3.1	3	3.4	3.1	3.3	2.6	1.8	1.339	0.9	1.3	1.339	1.41
Ho	0.95	1.2	1.3	1.3	1.1	1.7	0.98	0.8	1	0.64	0.62	0.7	0.6	0.7	0.5	0.3	0.25	0.2	0.3	0.25	0.24
Er	2.8	3.4	3.9	4.1	3.3	4.9	3	2.5	3.1	2	1.9	2	1.9	2	1.5	1.1	0.8	0.5	0.8	0.786	0.79
Tm	0.43	0.51	0.6	0.6	0.5	0.7	0.4	0.4	0.5	0.3	0.3	0.3	0.3	0.3	0.2	0.2	0.12	0.08	0.12	0.116	0.12
Yb	2.8	3.4	3.8	3.7	3.4	4.6	2.8	2.6	3.1	1.9	1.9	2	1.9	2	1.5	1.2	0.7	0.5	0.8	0.711	0.71
Lu	0.6	0.53	0.6	0.6	0.52	0.75	0.47	0.4	0.48	0.29	0.31	0.31	0.29	0.31	0.22	0.2	0.1	0.08	0.12	0.111	0.13
HREE	16.78	20.84	22.5	23.8	20.3	28.6	17.5	15.3	19.2	11.7	11.5	12.6	11.6	13.0	9.8	6.8	5.2	3.4	5.0	5.165	5.263
LREE/HREE	7.48	7.21	7.8	6.9	7.4	5.5	7.3	8.2	7.6	8.4	8.7	7.3	7.9	8.4	8.3	11.5	8.8	8.4	7.8	8.78	8.65
ΣREE	142.35	171.19	197.5	187.4	171.1	185	145.7	141.4	164.2	110.6	111.4	105.1	102.6	122.01	91.2	84.6	50.5	31.4	44.4	50.50	50.79
[La/Yb]N	7.56	7.55	7.7	7.5	7.5	5.5	7.5	8.2	7.8	9.1	8.9	8	8.1	9.2	8.7	12.97	9.97	9.9	8.25	9.97	9.80
[Gd/Yb]N	1.21	1.36	1.2	1.4	1.3	1.2	1.3	1.2	1.3	1.4	1.4	1.4	1.3	1.6	1.5	1.2	1.9	1.5	1.4	1.87	1.89
Eu/Eu*	0.65	0.68	0.62	0.65	0.64	0.64	0.66	0.62	0.59	0.57	0.63	0.62	0.65	0.65	0.62	0.63	0.72	0.52	0.6	0.70	0.69